PCCP

Analysis of transition state stabilization by non-covalent interactions in organocatalysis: Application of atomic and functional-group partitioned symmetry-adapted perturbation theory to the addition of organoboron reagents to fluoroketones

Journal:	*Physical Chemistry Chemical Physics*
Manuscript ID	CP-ART-03-2018-002029.R2
Article Type:	Paper
Date Submitted by the Author:	30-May-2018
Complete List of Authors:	Bakr, Brandon; Georgia Institute of Technology, Sherrill, C. David; Georgia Institute of Technology, School of Chemistry and Biochemistry

Analysis of transition state stabilization by non-covalent interactions in organocatalysis: Application of atomic and functional-group partitioned symmetry-adapted perturbation theory to the addition of organoboron reagents to fluoroketones

Brandon W. Bakr[1] and C. David Sherrill[1, 2, a)]

[1)] *Center for Computational Molecular Science and Technology, School of Chemistry and Biochemistry, Georgia Institute of Technology, Atlanta, GA 30332-0400*

[2)] *School of Computational Science and Engineering, Georgia Institute of Technology, Atlanta, GA 30332-0280*

(Dated: 30 May 2018)

This work seeks to apply symmetry-adapted perturbation theory (SAPT) to the recent study of Hoveyda and co-workers [K. A. Lee *et al., Nat. Chem.* 2016, **8**, 768] where an allyl addition to a ketone became enantioselective when the ketone was fluorinated. Through the application of atomic SAPT (A-SAPT) and functional-group SAPT (F-SAPT), the non-covalent interactions between specific atoms and functional groups in the transition states associated with the fluoroketone reactions can be quantified. Our A-SAPT analysis confirms that a H $\cdots$ F contact thought to enhance stereoselectivity shows a strong preference for one of the transition states leading to the experimentally observed product enantiomer. Other key atom-atom contacts invoked to rationalize relative transition state energies are also found to behave as expected based on chemical intuition and contact distances. On the other hand, hypothesized steric clashes between substrate phenyl or *ortho*-methyl phenyl groups and the catalyst are not supported by F-SAPT computations, and indeed, these are actually favorable π-π interactions.

[a)] Electronic mail: sherrill@gatech.edu

I. INTRODUCTION

In the activation-strain[1] or distortion-interaction[2] models, transition state (TS) barrier heights are the sum of the deformation energy penalties the reactants must pay to adopt the TS structure and the non-covalent interaction energy between the reactants. Design of more effective catalysts would be aided by a better understanding of these contributions to the energy. Indeed, several recent studies have explored the idea of improving the selectivity of organocatalytic reactions by tuning non-covalent interactions in the transition state.[3–8]

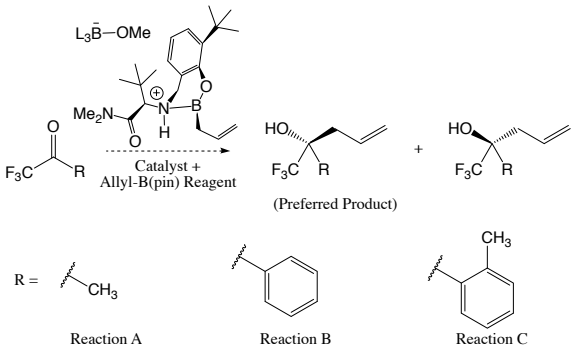

FIG. 1. Enantioselective addition of an allyl group to fluoroketones, through a complex formed between the allyl-boron reagent and an aminophenol catalyst.

Recently, Hoveyda and co-workers[9] hypothesized that electrostatic interactions between a positively charged ammonium moiety and a fluorine atom on the substrate could enhance enantioselectivity in the addition of allyl and allenyl groups to fluoroketones in reactions like those in Figure 1. The catalyst is generated by reacting an aminophenol molecule with an organoboron reagent bearing the allyl or allenyl group to be added, and reactions using several different trifluoro-methyl ketone substrates were examined. Density functional theory (DFT) was used to locate possible TS structures for the simplest substrate, 1,1,1-trifluoroacetone (reaction A of Figure 1), and the lowest-energy TS was one that featured the hypothesized H $\cdots$ F interaction. When experiments were performed using a variety of trifluoroketone substrates, the desired enantiomer was obtained with a high enantiomeric excess in most cases. For example, substrate 2,2,2-trifluoroacetophenone (reaction B in Figure 1) led to an enantiomeric ratio of 96:4. This contrasts with an enantiomeric ratio of 32:68 (i.e., the other enantiomer is preferred) for the non-fluorinated substrate. Both the DFT and experimental results are consistent with the hypothesis that H $\cdots$ F interactions

help stabilize the transition states leading to the desired products.

To rationalize the relative energies of the possible TS's, Hoveyda et al.[9] invoked various additional non-covalent interactions shown in Figure 2, based on the TS geometries and chemical intuition. We recently reported[10] a quantum mechanical study on the Houk-List mechanism for intermolecular aldol additions showing that chemical intuition is not necessarily reliable for understanding how non-covalent interactions might stabilize or destabilize the transition state. The original hypothesis for the origin of the stereoselectivity in that reaction was that the TS leading to the dominant product is stabilized by a favorable $NCH^{\delta+}\cdots^{\delta-}O{=}C$ H-bonding contact. However, direct computation of the strength of this contact using functional-group symmetry-adapted perturbation theory (F-SAPT)[11] showed that this is in fact a destabilizing interaction (due to repulsion between negative partial charges on the N and O atoms), and its strength in the possible transition state structures does not correlate with the observed product ratios.

In this paper, we seek to quantify the various non-covalent interactions that Hoveyda et al.[9] suggest are important in stabilizing or destabilizing the transition state structures for the organoboron catalyzed addition of an allyl unit to a fluoroketone substrate. We use F-SAPT and also the atomic version, A-SAPT.[12] Unlike our previous study of the Houk-List mechanism, here we find that chemical intuition about the nature of these contacts is mostly supported by the A-SAPT and F-SAPT analysis.

II. THEORETICAL METHODS

Symmetry-adapted perturbation theory[13] (SAPT) decomposes the interaction energy between two monomers in terms of electrostatics, exchange-repulsion, induction/polarization, and London dispersion forces.[13] Atomic SAPT (A-SAPT)[12] and functional-group SAPT (F-SAPT)[11] offer a more fine-grained analysis by partitioning densities to provide these same energetic components between interacting pairs of atoms or functional-groups of each monomer. These methods are based upon SAPT using Hartree–Fock monomer wavefunctions, with intermolecular interactions treated through second-order, and with intramolecular electron correlation neglected (sometimes abbreviated SAPT0). In this work, we use A-SAPT and F-SAPT to probe specific interactions between monomers in the transition state. These methods are used in combination with the jun-cc-pVDZ (jaDZ) basis set,[14]

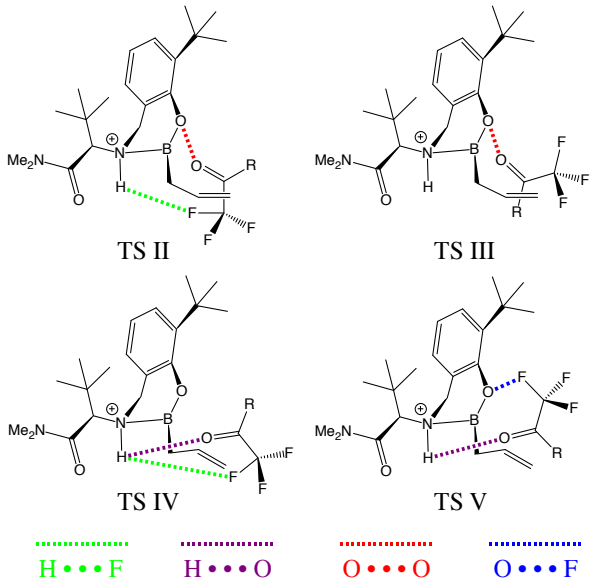

FIG. 2. Transition state structures for the reaction between trifluoro-methyl ketones and organoboron catalyst complexes from Figure 1, using the numbering from Ref. 9. Also shown are the non-covalent interactions suspected to determine the enantioselectivity of the reaction: repulsion between the oxygen of the carbonyl group of the fluoroketone and aryloxy oxygen of the catalyst complex in red; attraction between the carbonyl oxygen and the ammonium proton of the organoboron reagent in purple; attraction between a fluorine of the fluoroketone and the ammonium proton in green; repulsion of a fluorine of the fluoroketone and the aryloxy oxygen of the catalyst complex in blue.

which has been shown to provide reliable results when coupled with SAPT0.[15] Additionally, we use density fitted versions of these algorithms as implemented in Psi4[16–20] along with the appropriate auxiliary basis sets: the self-consistent field (SCF) procedure uses jun-cc-pVDZ-JK,[21] and the two-body contributions from SAPT0 (dispersion and exchange-dispersion) use jun-cc-pVDZ-RI.[22] Also, the core orbitals of heavy atoms are constrained to be doubly occupied, or "frozen," in all computations. For A-SAPT, we assign terms to atoms using iterative stockholder analysis (ISA) charges.[12,23] For F-SAPT, we use intrinsic bond orbital (IBO) local orbitals and charge analysis[24] together with a 50:50 "reduced" analysis of link bonds (assigning 50% of each link bond to its bordering fragments).[11] The A-SAPT and F-SAPT partitionings are constructed so that the SAPT components are recovered when summing over atoms or functional groups.

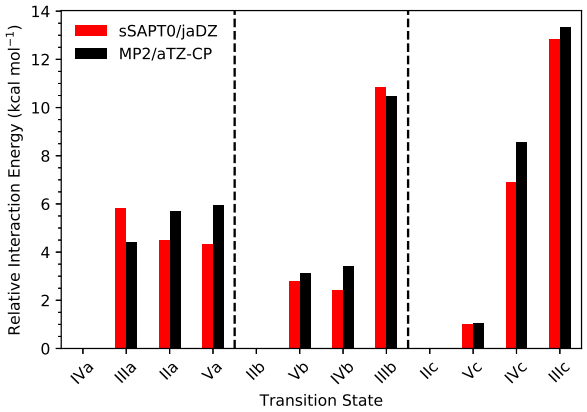

FIG. 3. Interaction energies are sorted by the strength of the counterpoise-corrected MP2/aTZ estimate within each reaction family (A, B, and C) and are plotted relative to the lowest interaction energy estimated within each model chemistry (exchange-scaled sSAPT0/jaDZ and MP2/aTZ).

Here, the monomers will be defined as the positively charged organoboron catalyst-complex, and the neutral fluoroketone substrate. We employed DFT transition state geometries reported by Hoveyda and co-workers,[9] and we use their naming scheme, in which the transition states are labeled II-V, with II and IV leading to the experimentally favored product enantiomer (see Fig. 2). A letter a–c after a TS label indicates a particular reaction, A, B, or C, as shown in Fig. 1.

SAPT0 provides unusually large induction and dispersion components for closely interacting systems, such as a doubly hydrogen bonded complex or a transition state.[10,15,25] This breakdown is due to the perturbative approach underlying SAPT and also a breakdown of the single-exchange (S^2) approximation used in computing the exchange-induction and exchange-dispersion terms.[25] In our previous study of non-covalent stabilization of transition states in proline-catalyzed aldol reactions,[10] we found that exchange-scaled SAPT (sSAPT) provided substantially improved results, consistent with its superior performance for other strongly-interacting systems like doubly hydrogen-bonded systems.[15,25] To examine the quality of the SAPT interaction energies for the systems of this study, ranging from 73–83 atoms, we have chosen to use counterpoise corrected (CP)[26] second-order Møller-Plesset perturbation theory (MP2)[27], with Dunning's correlation-consistent aug-cc-pVTZ basis set (aTZ)[28] as our benchmark.

As in our previous study applying F-SAPT to transition states,[10] exchange-scaling gen-

erally improves relative interaction energies, as seen in Figure S3. With exchange-scaling, sSAPT relative and absolute interaction energies differ by at most 1.9 kcal mol^{-1} (as seen in Figure 3) and 7.9 kcal mol^{-1}, respectively, from CP-corrected MP2/aTZ results for the systems studied, which have large total interaction energies in the range 37–60 kcal mol^{-1}. One might be concerned that MP2/aTZ could overbind some of the transition states due to the presence of π-π interactions;[29] we additionally checked that MP2/aTZ results for such transition states are in good agreement with ωB97X-V (Ref. 30), which is generally accurate for non-covalent interactions including π-π interactions.[31] These comparisons are presented in the Supporting Information for the interested reader.

An exchange-scaled version of A-SAPT has been implemented in a developer's version of Psi4 as described previously for F-SAPT.[10] It must be noted that the energetic quantities provided by SAPT or its A-SAPT or F-SAPT variants, e.g., the electrostatic interaction between a substrate fluorine and a hydrogen of the catalyst, cannot be directly observed by experiment; nevertheless, this type of analysis has been shown to effectively illuminate interaction motifs, such as hydrogen bonding and C–H/π interactions.[10–12,32]

III. RESULTS AND DISCUSSION

Hoveyda and co-workers obtained TS's for several substrates, including reactions A–C from Figure 1. Transition states II and IV lead to the preferred enantiomer of the product, while transition states III and V lead to the opposite enantiomer. For reaction A, IV is the lowest-lying TS, with II and V lying 2.6–3.7 kcal mol^{-1} higher in energy [depending on the density functional, either M06-2X or ωB97X-D with a 6-311++G(2df,2pd) basis].[33,34] III lies higher still, at 5.5 kcal mol^{-1} above IV. Reaction B, with R = phenyl, features similar energetics, but II and V are slightly closer in energy to IV (lying 1.5–3.2 kcal mol^{-1} higher), and III is slightly destabilized (7.6–8.3 kcal mol^{-1} above IV). For reaction C, II and IV are closer to each other (within 1.2 kcal mol^{-1}), and which is lower depends on the functional used. V lies slightly higher at 1.4–1.8 kcal mol^{-1}, while III lies substantially higher (7.1–8.3 kcal mol^{-1}). In all cases, either transition state IV or II, both of which lead to the preferred product, are found to be the lowest in energy.

These TS relative energies are rationalized by Hoveyda and co-workers primarily on the basis of various stabilizing or destabilizing non-covalent interactions (although of course

distortion energies also play a role in determining the total TS energies). The key H $\cdots$ F interaction thought to engender enantioselectivity (in green, Figure 2) is hypothesized to stabilize both II and IV, which both lead to the preferred product. This contact should be stronger in II than IV because the distance between the H and F atoms is $\sim$ 2.0 Å in II, but $\sim$ 4.1 Å in IV. However, IV lies energetically below II for reactions A and B, and possibly for reaction C (depending on the functional used). Hoveyda and co-workers hypothesize that II is destabilized relative to IV because of an electrostatic repulsion between the carbonyl oxygen and the aryloxy oxygen of the catalyst complex (O $\cdots$ O interaction in red, Figure 2).

Hoveyda and co-workers hypothesize that TS's III and V lie higher in energy than II and IV because they lack the stabilizing H $\cdots$ F contact, and also because they feature repulsive interactions between the aryloxy oxygen of the catalyst complex and either the carbonyl oxygen (O $\cdots$ O contact in red in Fig. 2, for III) or a fluorine (O $\cdots$ F contact in blue in Fig. 2, for V). Finally, the transition states are thought to be stabilized by a favorable electrostatic contact between the carbonyl oxygen and the ammonium proton (H $\cdots$ O contact in purple in Figure 2). This contact is expected to be more favorable in TS's V and IV than in II and III, due to a shorter H $\cdots$ O distance, and this is expected to be one reason why V lies lower in energy than III.

In addition to atom-atom contacts, steric interactions between the organoboron catalyst and bulkier R-groups (benzene and *o*-methylbenzene) of the substrate are expected to play a role in altering the enantioselectivity of reactions B and C. As a result of the steric clashing, the substrate is expected to deform into a higher energy geometry in the transition state as well. Hoveyda and co-workers argue that these two effects combine to reduce the preference for TS IV in reaction B and completely eliminate the preference for TS IV in reaction C (with TS II becoming essentially isoenergetic).[9]

In the following discussion, we will analyze the aforementioned interactions hypothesized by Hoveyda and co-workers to determine the enantioselectivity of reactions A–C. For the atom-atom interactions, this will be done within the A-SAPT model, and functional group interactions will be assessed using the F-SAPT model. Figures 4–6 show the A-SAPT predicted energetics for the interactions under study in Reactions A–C, in terms of the usual SAPT decomposition: electrostatics, exchange-repulsion, induction/polarization, and London dispersion. Note that some of the atom-atom partitions of the induction energy can be positive (repulsive), even though the *total* induction energy must be negative (attractive);

the polarization of electron density acts on the whole to stabilize the complex, but that does not imply that the polarization stabilizes every constituent interatomic contact.[12]

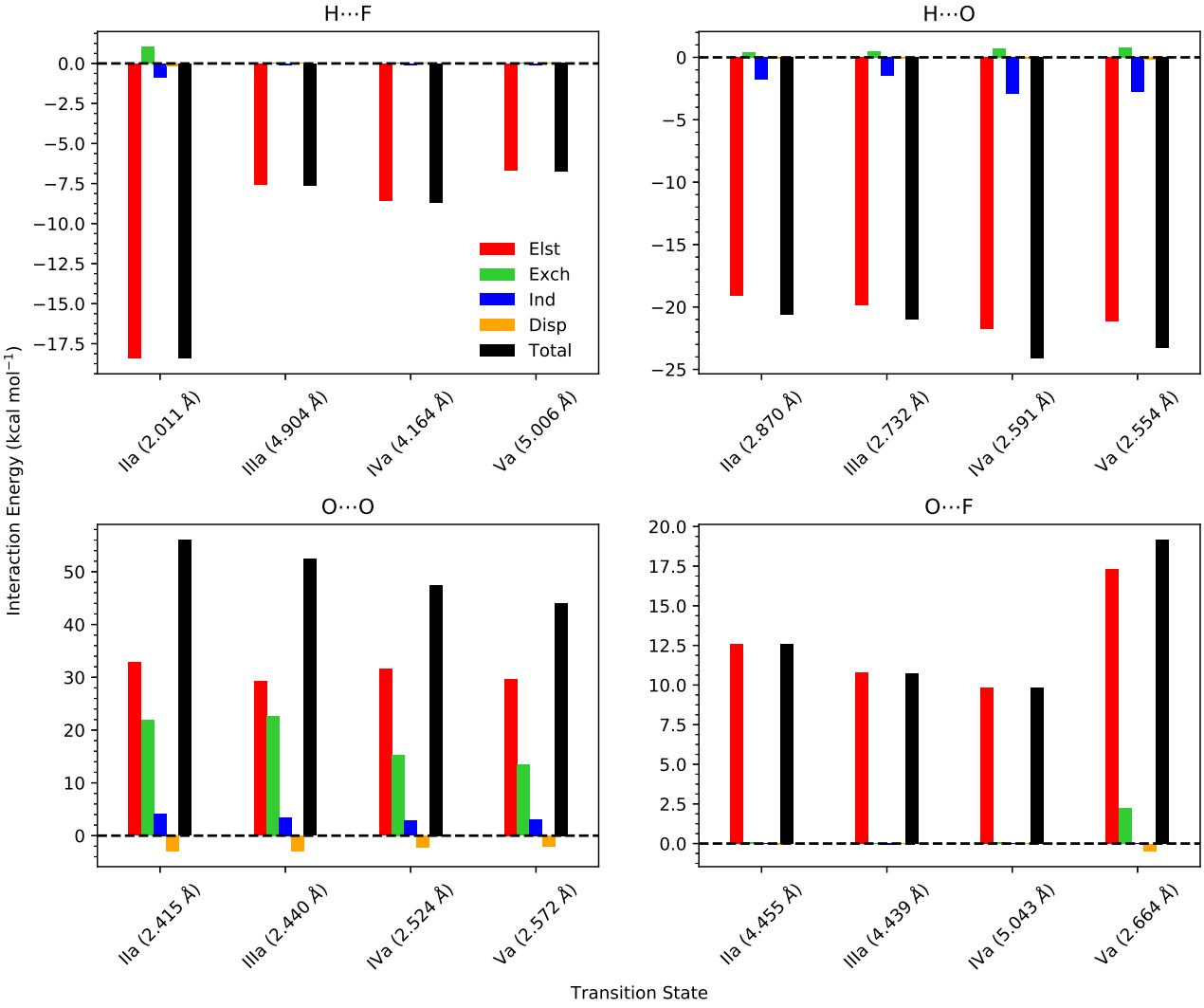

FIG. 4. Exchange-scaled A-SAPT/jaDZ analysis of the interactions in transition states for Reaction A in terms of electrostatics, exchange-repulsion, induction, and dispersion. Each panel corresponds to an atom-atom interaction depicted in Figure 2.

A. H ··· F

Hoveyda and co-workers note that the H ··· F interaction is most pronounced in TS II by virtue of it having the closest contact ($\sim$ 2.0 Å), but is also close enough ($\sim$ 4.1 Å) to exhibit a substantial stabilizing effect in IV. Both of these TS's lead to the preferred product

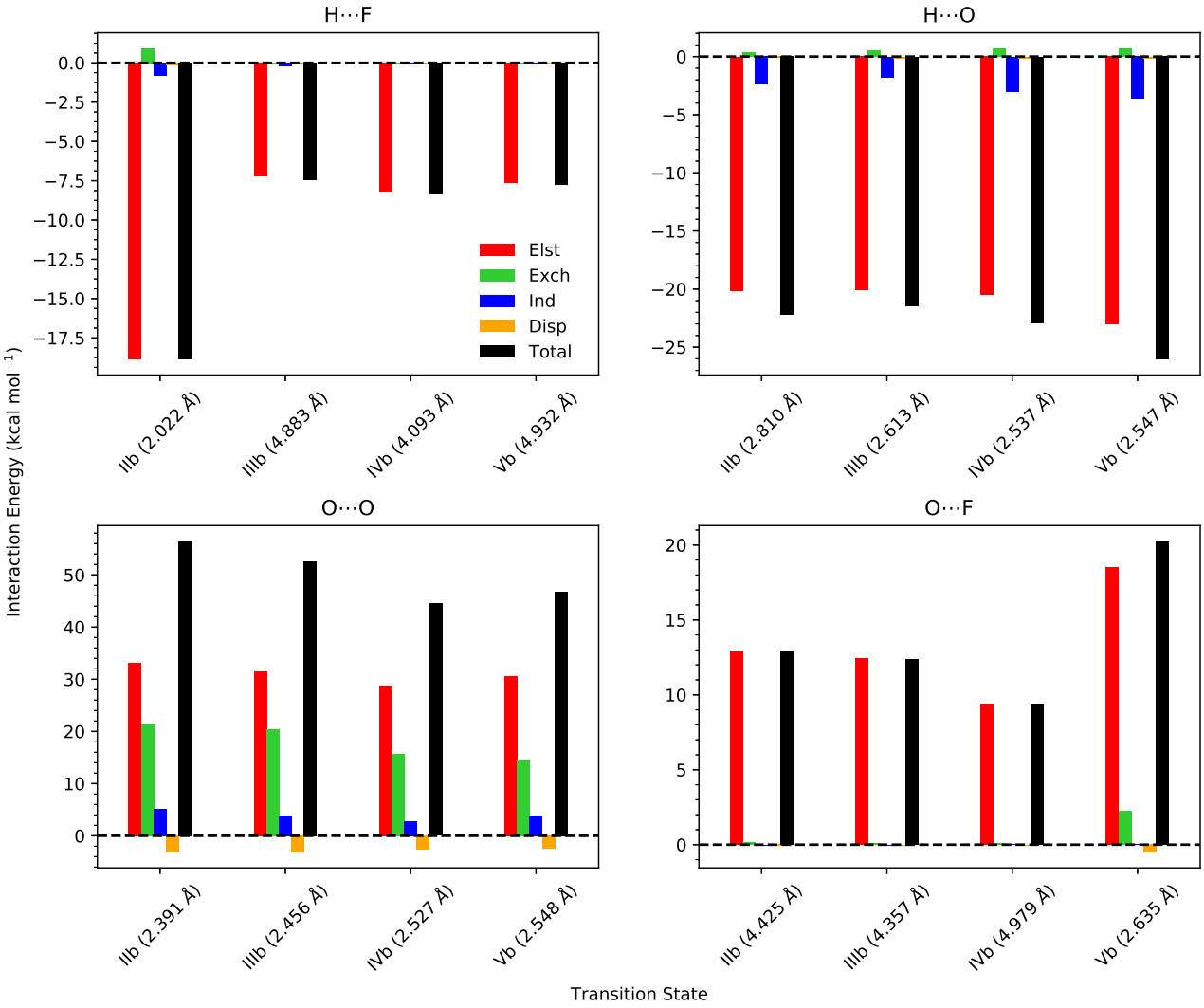

FIG. 5. Exchange-scaled A-SAPT/jaDZ analysis of the interactions in transition states for Reaction B in terms of electrostatics, exchange-repulsion, induction, and dispersion. Each panel corresponds to an atom-atom interaction depicted in Figure 2.

enantiomer.

As seen in Figures 4–6, A-SAPT indicates that the H $\cdots$ F total interaction is indeed most stabilizing in II, followed by IV, as predicted by Hoveyda and co-workers. This interaction is dominated by electrostatics in all TS's. In fact, II is the only TS to have noticeable contributions from components other than electrostatics. With respect to electrostatics, II is stabilized by 18–20 kcal mol^{-1} and IV is stabilized by 7–9 kcal mol^{-1} across reactions A–C, making II the most stabilized from this interaction by far, as expected from having the closest contact distance by more than a factor of two. III and V are slightly less stabilized by

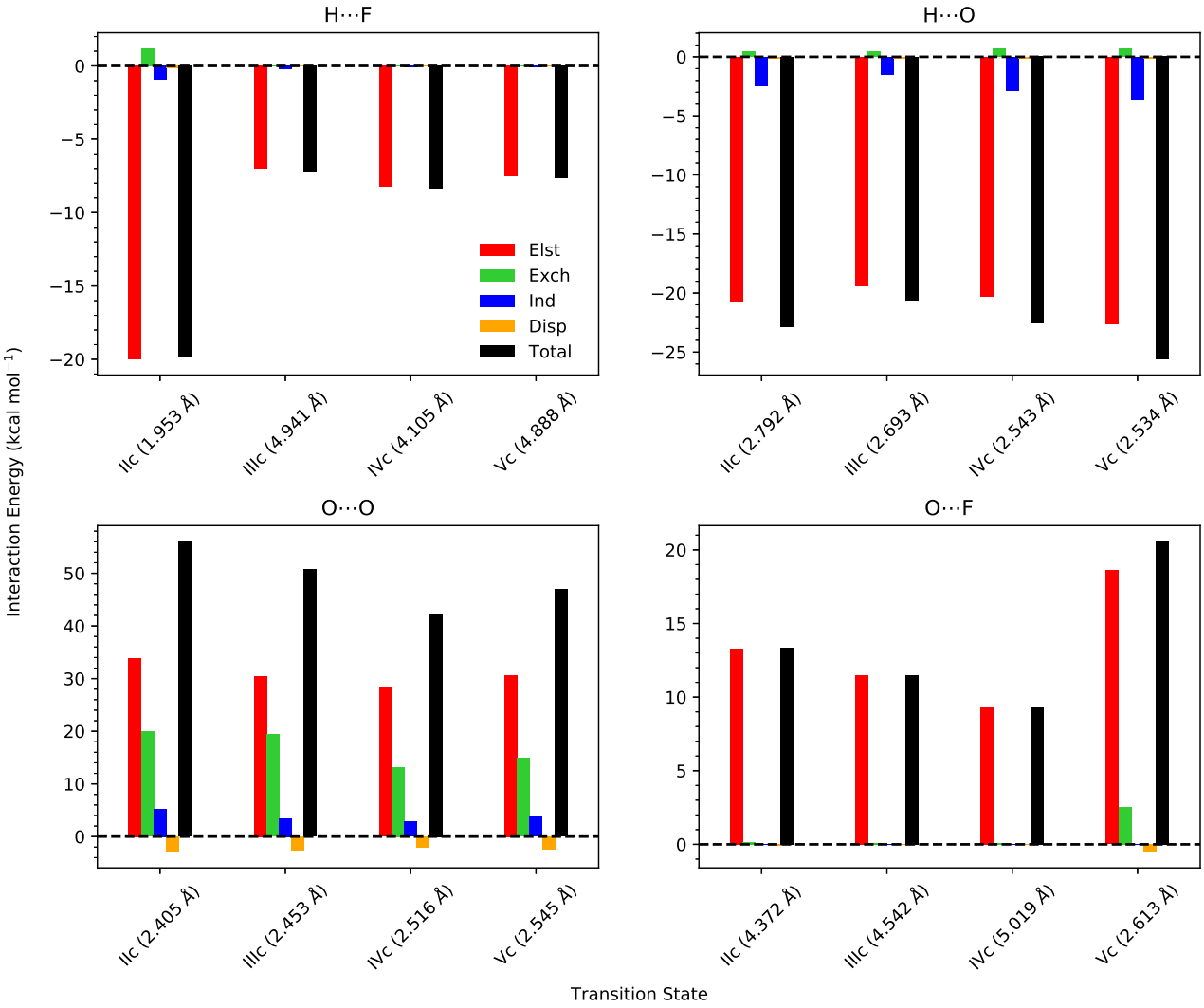

FIG. 6. Exchange-scaled A-SAPT/jaDZ analysis of the interactions in transition states for Reaction C in terms of electrostatics, exchange-repulsion, induction, and dispersion. Each panel corresponds to an atom-atom interaction depicted in Figure 2.

this contact than IV, due to their larger contact distances (0.7–0.8 Å longer). In this case, A-SAPT confirms chemical intuition that the energetics of this contact should correlate with distance. Although II has the shortest distance and thus greatest stabilization due to this contact, Figure 3 indicates that IV is overall more stabilized by non-covalent interactions in the case of reaction A. This indicates that other contacts are also significant in determining the TS energetics.

B. H ··· O

Hoveyda and co-workers imply that TS's IV and V should exhibit the strongest H ··· O interaction because the chair conformation allows for a shorter contact distance. The authors suggest that this contact is one of the reasons that IV lies energetically below II. In all TS's of reactions A–C, the electrostatics component of the interaction is dominant and stabilizing by 19–23 kcal mol^{-1}, while induction is a slightly stabilizing component (1–3 kcal mol^{-1}). The exchange-repulsion component is slightly destabilizing ($<$ 1 kcal mol^{-1}), and dispersion is negligible.

TS's IV and V are clearly the most stabilized by this contact for reaction A, as expected by Hoveyda and co-workers on the basis of the contact distances (however, TS IV is slightly more stabilized despite a slightly longer distance, 2.59 vs 2.55 Å). V is the most stabilized TS in reactions B and C, despite having a longer contact distance than IV in reaction B (2.55 vs 2.54 Å). The contact in II becomes similarly stabilized as in IV for reactions B and C despite not having the chair conformation, and thus featuring a longer contact distance (about 2.80 Å in both reactions vs about 2.54 Å in IV). In reaction C, II is actually more stabilized by this interaction than IV. Across all three reactions, the hypothesis that V is stabilized relative to III by the H ··· O contact is supported by the A-SAPT analysis.

C. O ··· O

The aryloxy oxygen and carbonyl oxygen contact represents a close (2.39–2.57 Å), destabilizing interaction for all transition states of reactions A–C. However, it is expected to be more destabilizing in II and III due to a slightly closer contact distance (2.39–2.46 Å) in these TS's as compared to IV and V (2.52–2.57 Å). The O ··· O interaction is destabilizing by more than 40 kcal mol^{-1} across all examined TS's and is dominated by electrostatics (consistently around 30 kcal mol^{-1}). There are also considerable contributions from exchange-repulsion, which are markedly more destabilizing for TS's II and III (19–23 kcal mol^{-1}) than IV and V (13–16 kcal mol^{-1}) for reactions A–C. Induction/polarization and London-dispersion are relatively negligible components of all the O ··· O interactions, accounting for around 3–5 kcal mol^{-1} destabilization and around 2–3 kcal mol^{-1} stabilization, respectively.

As a result of the difference in exchange-repulsion, the total O ··· O interaction of IV

and V (42–48 kcal mol^{-1}) is substantially less destabilizing than in II and III (51–57 kcal mol^{-1}) across all of the reactions. This difference in destabilization predicted by A-SAPT is consistent with Hoveyda and co-workers' hypothesis that the O $\cdots$ O interaction causes II to be energetically higher than IV for reactions A and B. Although the trends of this interaction remain the same for reaction C, the total DFT energy of IIc is either slightly lower than that of IVc, or very slightly higher, depending on the density functional employed,[9] which suggests that other factors must contribute to the energetic ordering for that reaction.

D. O $\cdots$ F

Repulsion between the aryloxy and fluorine in Va is hypothesized by Hoveyda and co-workers to make it less preferred than IVa, despite Va having presumably similar O $\cdots$ O and H $\cdots$ O interactions to IVa. This difference is expected due to the distance of the contact in V being around 2.7 Å, and over 4.4 Å for the other TS's, with IVa having the longest contact distance by a margin of $\sim$ 0.5 Å (similar distances are seen in reactions B and C). Indeed, in reactions A–C, A-SAPT reflects Hoveyda and co-workers' expectations: TS IV minimizes the destabilizing effect of the O $\cdots$ F interaction (9–10 kcal mol^{-1}) and V maximizes the destabilization (19–21 kcal mol^{-1}).

Across all reactions, the electrostatic component is destabilizing (9–13 kcal mol^{-1} for II, III, and IV, and 17–19 kcal mol^{-1} for V). This is the only significant component of the interaction except in TS V, where the atoms are close enough for exchange-repulsion to become a minor contributor (2–3 kcal mol^{-1}). Thus, the A-SAPT results confirm the hypothesis that the O $\cdots$ F contact is destabilizing in V compared to IV or the other TS's.

Thus, the present A-SAPT analysis of the H $\cdots$ F, H $\cdots$ O, O $\cdots$ O, and O $\cdots$ F contacts are all consistent with the rationalizations of the DFT relative energies of the transition states reported by Hoveyda and co-workers.[9]

E. Steric Interactions in Reaction B

In reaction B, the methyl substituent of the fluoroketone substrate is replaced with a phenyl group. The DFT energies computed by Hoveyda and co-workers show that TS IV is now only 1.5–2.8 kcal mol^{-1} below II, compared to 2.6–3.3 kcal mol^{-1} for reaction A.

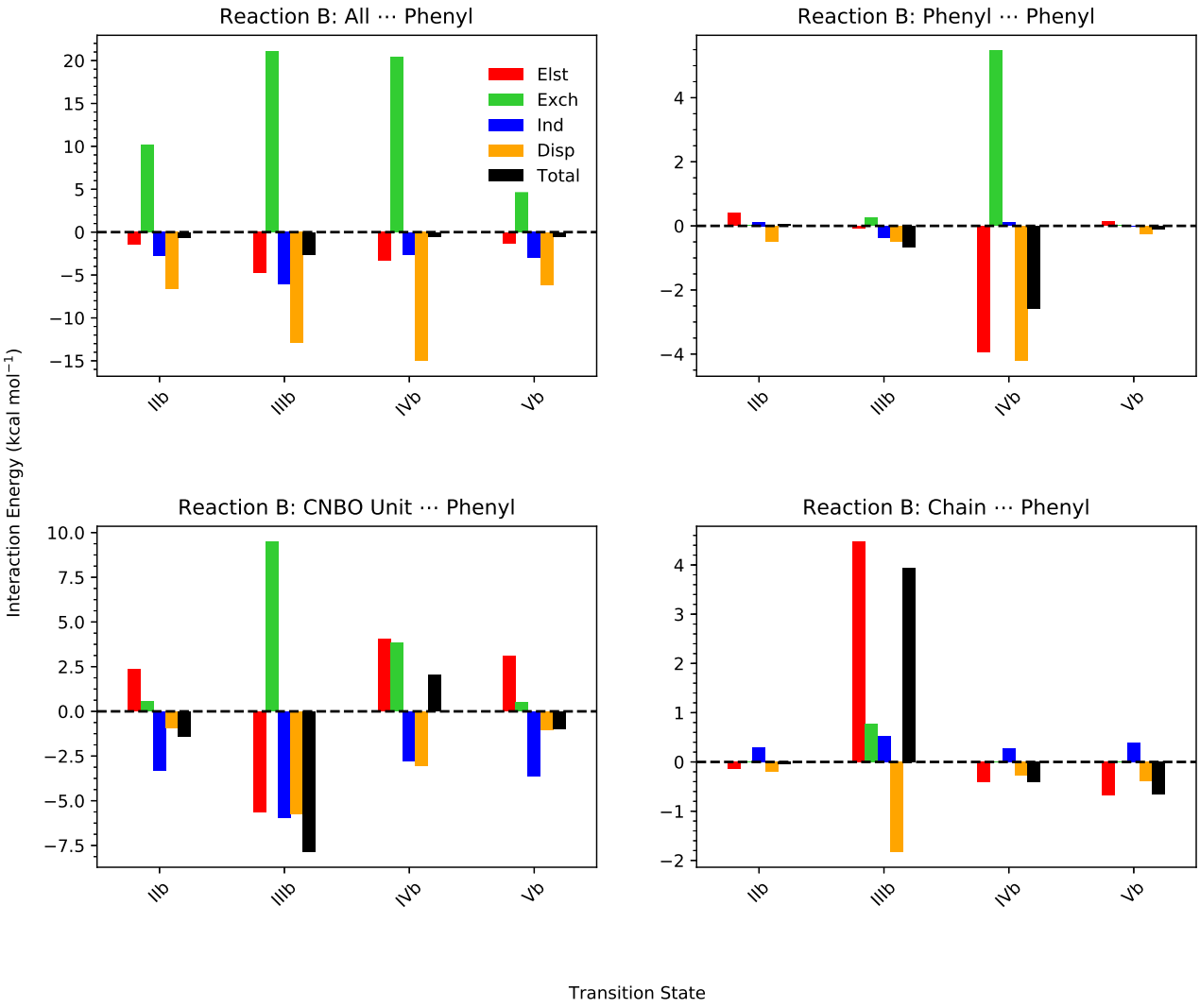

FIG. 7. Exchange-scaled F-SAPT/jaDZ analysis of various interactions between the whole organoboron catalyst, phenyl, CNBO "chair", and the $(Me)_2$N-CO-CH-*t*-butyl "chain" of the organoboron catalyst with the phenyl of the substrate in transition states for Reaction B in terms of electrostatics, exchange-repulsion, induction, and dispersion.

They rationalize the decreased preference for TS IV by citing potentially destabilizing steric interactions between the bulk of the catalyst complex and the newly introduced phenyl group of the fluoroketone substrate. This hypothesis is supported by distortion of the carbonyl to phenyl O=C-C-C dihedral angle (32° out of plane) in the substrate, which contributes to the removal of favorable π conjugation between the phenyl group and the carbonyl in TS IVb.

F-SAPT analysis shows that the interaction of the phenyl group of the substrate with the

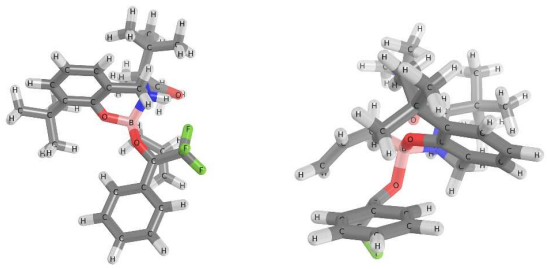

FIG. 8. The π faces of IIb (left) do not align as favorably for π-π interactions as they align in IVb (right).

catalyst complex is slightly less favorable in IVb (-0.5 kcal mol^{-1}) than IIb (-0.6 kcal mol^{-1}) as seen in the top left panel of Figure 7; this is in accord with the expectations of Hoveyda and co-workers, but the energy difference is very small. Comparing the interaction between the phenyl group of the substrate and the phenyl group of the catalyst complex, shown in the top right panel of Figure 7, the exchange-repulsion is larger in IVb (5.5 kcal mol^{-1}) than in IIb (0.4 kcal mol^{-1}), as expected due to the much closer center of mass distance between the phenyl rings in IV (4.78 Å vs 6.73 Å). However, the structure of IVb places the closer phenyl rings in a favorable geometry for a π-π interaction, as shown in Figure 8 (the geometry is intermediate between an offset-stacked and a tilted T-shaped configuration), while the structure of IIb features a longer distance and poor relative orientation for a π-π interaction.

This favorable π-π geometry in IVb leads to stabilizing electrostatic contributions of 4.0 kcal mol^{-1} and London dispersion stabilization of 4.2 kcal mol^{-1} that overcome the higher exchange repulsion, leading to an overall phenyl-phenyl interaction energy of -2.6 kcal mol^{-1} in IVb. In IIb, the electrostatic component is destabilizing by 0.4 kcal mol^{-1}, and London dispersion is stabilizing by 0.5 kcal mol^{-1} for the phenyl-phenyl interaction. This results in a total phenyl-phenyl interaction that is nearly zero (0.1 kcal mol^{-1}) in IIb. Thus, with regard to the phenyl-phenyl interaction, Hoveyda and co-workers are correct that the exchange-repulsion term is larger in IVb than IIb, but one might not have expected that a favorable π-π interaction will overcome this repulsion.

The interaction between a *t*-butyl substituent of the phenyl group on the catalyst and the phenyl of the substrate presents another possibility for increased steric repulsion in TS IVb relative to IIb. However, F-SAPT analysis shows this interaction in IVb is overall

attractive (-0.8 kcal mol^{-1}) due to attractive electrostatic and dispersion terms overcoming a large, destabilizing exchange-repulsion term (4.2 kcal mol^{-1}). The same interaction in IIb is similarly stabilizing (-0.6 kcal mol^{-1}); however, individual components in this case are quite small because of the greater separation between the *t*-butyl and the phenyl group.

The phenyl group of the fluoroketone substrate also has significant interactions with the central CNBO "chair" of the catalyst in both IIb and IVb, as seen in the bottom left panel of Figure 7. In fact, among interactions involving the substrate phenyl, this interaction makes the largest difference towards destabilizing IV compared to II as one moves from Reaction A to reaction B (it shifts the relative interaction energies by 4.1 kcal mol^{-1}). In IVb, there is a close contact (2.39 Å) between a hydrogen of the substrate phenyl and a hydrogen of the chair unit, leading to significant destabilizing exchange-repulsion and electrostatic terms. In IIb, the closest phenyl–CNBO contact is much more distant (3.27 Å), reducing the unfavorable interactions and yielding an overall 3.4 kcal mol^{-1} interaction energy preference for IIb over IVb. By contrast, in Reaction A, the CNBO chair / substrate methyl interaction is much more similar in IIa and IVa, and IVa is actually slightly preferred by this interaction (by 0.7 kcal mol^{-1}).

The most significant remaining interaction involving the substrate phenyl group is a rather unfavorable electrostatic interaction between the phenyl group and the $(Me)_2$N-CO-CH-*t*-butyl "chain" of the catalyst, which further destabilizes the relative interaction energy of IIIb compared to what it was in IIIa (by about 4 kcal mol^{-1}, see bottom right panel of Figure 7).

Finally, although it does not directly involve the substrate R group (methyl or phenyl), we note that the catalyst chair / substrate carbonyl interaction is significantly less stabilizing in IVb relative to IIb (-3.9 kcal mol^{-1}) than it was in IVa relative to IIa (-8.3 kcal mol^{-1}, see Supporting Information). This interaction includes the incipient bond formation between the catalyst boron atom and the carbonyl oxygen of the substrate, which involves large energy components. IVa and IVb feature similar contact distances (1.59 and 1.58 Å, respectively), and IVb is 4.0 kcal mol^{-1} more stabilized by this contact than IVa (although the difference is only about 9% for this large interaction energy). By contrast, the geometry of IIb allows for a much closer contact (1.54 Å) than is possible in IIa (1.62 Å), meaning that the improvement in the interaction energy of IIb vs. IIa is much larger (8.4 kcal mol^{-1}). Thus, differences in the transition state geometries mean that the catalyst chair / substrate carbonyl interaction

also contributes to the decreased preference of TS IV vs TS II as one moves from Reaction A to Reaction B.

To summarize this section, we have investigated a hypothesis of Hoveyda and co-workers[9] to explain why the DFT energy gap between TS's IV and II is reduced by 0.5–1.1 kcal mol^{-1} in Reaction B compared to Reaction A. Those researchers suggested that the decreased preference for IV is due to larger steric repulsions between the catalyst and the substrate, due to the larger R group in Reaction B (phenyl) compared to reaction A (methyl). The expected steric clash between the phenyl of the substrate and the phenyl of the catalyst is, contrary to prior expectations, *stabilizing* in TS IVb due to a favorable π-π interaction. Likewise, the substrate phenyl has favorable interactions with the *t*-butyl group off the catalyst phenyl (which are similar in magnitude for TS's IVb and IIb). The biggest direct contributor to the destabilization of IVb vs IIb involving the substrate phenyl is the interaction of the substrate phenyl with the central CNBO chair of the catalyst, but this contribution is cancelled by the previously mentioned substrate phenyl interactions that are more favorable for IVb than IIb, so that the net phenyl $\cdots$ catalyst interactions are approximately equal for IVb and IIb. The most important change in the relative interaction energies of IV and II as one moves from Reaction A to Reaction B seems to be a change in the interaction between the catalyst CNBO chair and the substrate carbonyl, where IV shows a reduced preference over II in Reaction B compared to Reaction A, which is caused by a more favorable bond formation geometry in IIb compared to IIa.

Finally, we note that in terms of just interaction energies, IVb is 2.4 kcal mol^{-1} *less* stable than IIb, whereas IVa is 4.5 kcal mol^{-1} more stable than IIa (see Figure 3). The fact that IVb remains below IIb according to Hoveyda's DFT computations is attributed to differences in reactant distortion energies. Indeed, at the MP2/aTZ level of theory, we compute that the distortion energy of IIb is nearly 6 kcal/mol greater than that of IVb (see Figure S4 of the Supporting Information).

F. Steric Interactions in Reaction C

In reaction C, an *ortho*-methyl substituent has been added to the phenyl group of the substrate. Hoveyda and co-workers found that this addition reduced the enantiomeric ratio to 83:17, compared to 96:4 for Reaction B.[9] They hypothesized that the additional steric

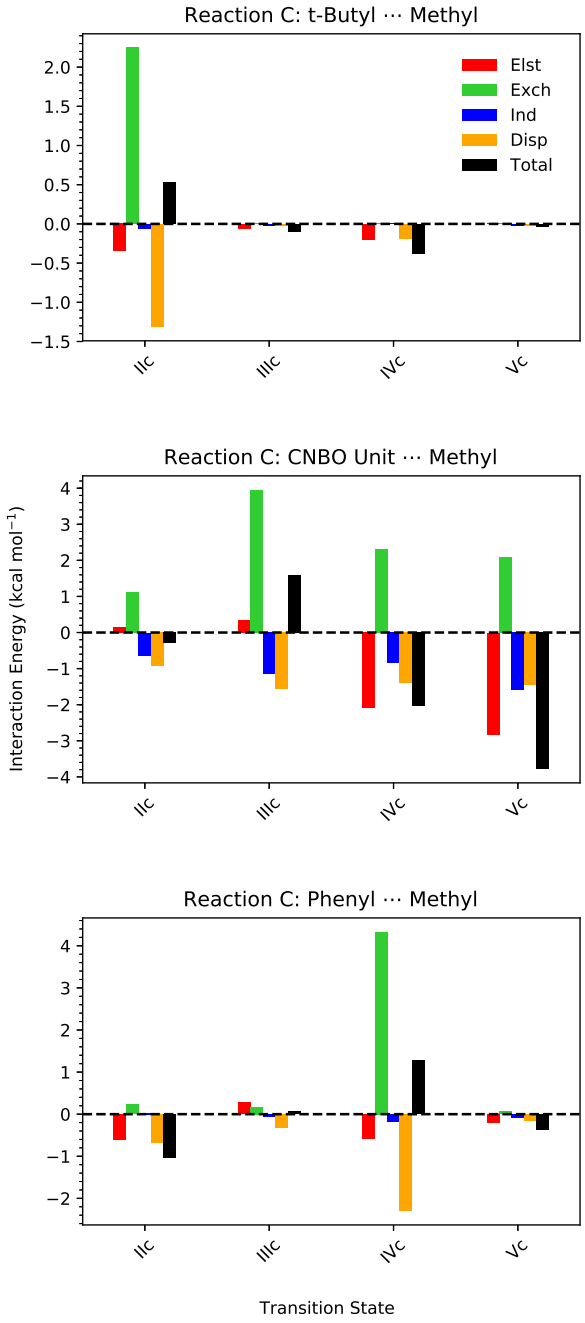

FIG. 9. Exchange-scaled F-SAPT/jaDZ analysis of various interactions between the *t*-butyl, phenyl, and CNBO "chair" of the organoboron catalyst with the *ortho*-methyl group of the substrate in transition states for Reaction C in terms of electrostatics, exchange-repulsion, induction, and dispersion.

bulk from the methyl group led to more repulsion between the substrate and the catalyst's phenol moiety, thus destabilizing the transition states (IIc and IVc) that lead to the preferred

enantiomer; the other two transition states (IIIc and Vc) orient the R group of the substrate away from the phenol group of the catalyst, and are not affected by the additional steric bulk of the methyl group. The DFT results tend to support this hypothesis. Transition state Vc is now only 1.4 or 1.8 kcal mol^{-1} (M06-2X or ωB97X-D) above the most stable transition state (either IIc or IVc, depending on the functional); in Reaction B, the gap is somewhat larger, 1.7 or 3.2 kcal mol^{-1}, respectively. This makes the non-preferred reaction pathway less unfavorable. (Transition state III remains higher in energy by several kcal mol^{-1}).

Moreover, the notion that this decreased preference for IIc and IVc relative to Vc is due to steric clashes between the R group of the substrate and the phenol moiety of the catalyst is supported by the transition state geometries. TS IVc demonstrates an even larger distortion away from planar conjugation for the carbonyl and phenyl groups of the substrate (O=C-C-C angle of $\sim 55^{o}$) than was seen for Reaction B ($\sim 32^{o}$). In TS IIc, there is a close 2.33 Å contact between the *ortho*-methyl substituent and the *t*-butyl group of the catalyst.

SAPT analysis supports the idea that TS's II and IV are destabilized relative to V as the *ortho*-methyl substituent is added to the substrate phenyl ring. As shown in Figure 3, for Reaction B, TS V has about the same amount of interaction energy stabilization as IV, while II has an additional 2–3 kcal mol^{-1} of stabilization. For Reaction C, the gap between II and V is reduced to only $\sim$ 1 kcal mol^{-1} (II remains more stable), while IV's interaction energy is now 7 kcal mol^{-1} less favorable than II's. (The fact that IVc's DFT energy is very similar to those of IIc and Vc, despite IVc having a much less stabilizing interaction energy, is due to its having a lower deformation energy than IIc and Vc; MP2/aTZ computations show that IIc and Vc have deformation energies $\sim$ 8 kcal mol^{-1} higher than IVc, see Figure S4 of the Supporting Information).

F-SAPT analysis provides more detailed information on the origins of these differences in non-covalent interaction energies. Here, we examine interactions between the *ortho*-methyl portion of the substrate vs the *t*-butyl, phenyl, and CNBO "chair" portions of the catalyst. The results are presented in Figure 9.

For the interaction of the *t*-butyl group off of the phenyl of the organoboron catalyst with the *ortho*-methyl of the substrate, IIc is expected to have the strongest destabilizing interaction due to it having the closest contact distance (2.33Å). Indeed, as seen in the top left panel of Figure 9, IIc has the most destabilizing interaction according to F-SAPT. However, the substantial 2.2 kcal mol^{-1} exchange repulsion for this contact is mostly canceled

by a -1.3 kcal mol^{-1} dispersion interaction; the overall contact including electrostatic terms also is repulsive by only 0.5 kcal mol^{-1}. This same interaction is negligible in IIIc and Vc, and is weakly stabilizing (-0.4 kcal mol^{-1}) in IVc.

A close contact between the phenyl group of the organoboron catalyst and the *ortho* methyl of the substrate is expected to result in steric clashing for TS IVc (C $\cdots$ H distance of 2.51 Å). According to F-SAPT analysis (bottom panel, Fig. 9), the interaction is most destabilizing in IVc (1.3 kcal mol^{-1}). IIc's interaction is stabilizing by an almost equal magnitude (1.0 kcal mol^{-1}).

Though not explicitly mentioned by Hoveyda and co-workers, the CNBO unit of the organoboron catalyst appears to sterically clash with the *ortho*-methyl group in IIIc, contributing to the relative interaction energy of III being even higher in reaction C than it was in reaction B (see Figure 3). F-SAPT analysis confirms that IIIc is destabilized by this contact (by 1.6 kcal mol^{-1}), although IVc and Vc are substantially stabilized (by 2.1 kcal mol^{-1} and 3.8 kcal mol^{-1}, respectively, middle panel of Fig. 9). As anticipated, exchange-repulsion is the most destabilizing component of the interaction IIIc (4.0 kcal mol^{-1}), and is large enough to overcome the stabilizing dispersion and induction terms (which sum to 2.7 kcal mol^{-1}). IVc and Vc have significant electrostatic stabilization for this contact, with additional stabilizing dispersion and induction contributions. The significant stabilization of Vc by this contact contributes to the nearly equal interaction energies of IIc and Vc in Figure 3.

Overall, F-SAPT analysis supports the idea that steric clashes involving the methyl substituent on the substrate phenyl lead to a less favorable interaction energy of IVc relative to Vc. The *t*-butyl $\cdots$ *ortho*-methyl contact also destabilizes IIc vs Vc, but by a modest amount that is approximately canceled by a more favorable phenyl $\cdots$ methyl contact in IIc vs Vc. Perhaps surprisingly, favorable contacts between the methyl substituent and the CNBO "chair" of the catalyst are also substantially stabilizing for Vc vs the other transition states.

IV. CONCLUSIONS

Work by Hoveyda and co-workers revealed that the oraganoboron catalyzed allyl addition to a ketone substrate results in an enantioselective reaction upon adding fluorines to the

ketone substrate.[9] When acetophenone is the substrate, the preferred enantiomer is produced with low efficiency (32:68 e.r.); however, the fluorinated ketone (2,2,2-trifluoroacetophenone) produces the desired enantiomer through transition states II and IV in an enantioselective reaction (96:4 e.r.). Hoveyda and co-workers posit that this enhanced selectivity is due to the presence of a stabilizing electrostatic interaction between a fluorine of the ketone substrate and a nearby ammonium proton in the transition states leading to the dominant product. Additional non-covalent interactions are invoked to explain the relative energies of the transition states as obtained by density functional theory. The current work has analyzed these claims by direct quantification of non-covalent interactions using the atomic and functional group partitions of symmetry-adapted perturbation theory (A-SAPT and F-SAPT).

As hypothesized by Hoveyda and co-workers, A-SAPT confirms that there is a large stabilization of the transition states due to the non-covalent interaction between the substrate fluorine atom and the ammonium proton of the catalyst, and that this stabilization is much greater for one of the transition states (II) leading to the preferred enantiomer. This stabilization is almost entirely electrostatic in nature. Other atom-atom interactions proposed to influence the enantioselectivity of the reaction by Hoveyda and co-workers (carbonyl oxygen of the substrate interacting with the ammonium proton of the organoboron catalyst, the carbonyl oxygen interacting with a nearby oxygen in the CNBO unit of the organoboron catalyst, and the oxygen of the CNBO unit of the organoboron catalyst interacting with the nearest fluorine of the fluoroketone substrate) are also confirmed by our A-SAPT analysis.

We examined three reactions studied by Hoveyda and co-workers; in Reaction A, the R group of the trifluoro-methyl ketone substrate is a methyl group, whereas in Reactions B, and C, the methyl of the substrate is replaced by a phenyl group or an *ortho*-phenyl group, respectively. For reactions B and C, the bulkier R-group was expected to destabilize the transition states through steric clashing with the organoboron catalyst. However, F-SAPT analysis shows that this interaction is actually a stabilizing π-π interaction, and it contributes to the overall preference for TS IV.

Overall, this work has directly confirmed a majority of the non-covalent interactions that were thought to play a role in the enantioselectivity of the organoboron catalyzed allyl addition to a fluoroketone through the application of A-SAPT and F-SAPT. F-SAPT analysis suggests that some interactions that may be seen as sterically repulsive according

to chemical intuition are actually stabilizing when electrostatic and dispersion interactions are quantified. The results of this study suggest that these SAPT partitions can be used to directly assess the relative strengths on non-covalent interactions in future organocatalysis research.

ACKNOWLEDGMENTS

This work was supported by the U.S. Department of Energy, Office of Basic Energy Science, through catalysis contract No. DE-FG02-03ER15459, and by the U.S. National Science Foundation through grant CHE-1566192.

REFERENCES

[1]I. Fernández and F. M. Bickelhaupt, *Chem. Soc. Rev.*, 2014, **43**, 4953–4967.

[2]D. H. Ess and K. N. Houk, *J. Am. Chem. Soc.*, 2007, **129**, 10646–10647.

[3]E. H. Krenske and K. N. Houk, *Acc. Chem. Res.*, 2013, **46**, 979–989.

[4]S. E. Wheeler, T. J. Seguin, Y. Guan and A. C. Doney, *Acc. Chem. Res.*, 2016, **49**, 1061–1069.

[5]T. J. Seguin and S. E. Wheeler, *ACS Catal.*, 2016, **6**, 7222–7228.

[6]T. J. Seguin and S. E. Wheeler, *Angew. Chem. Int. Ed.*, 2016, **55**, 15889–15893.

[7]Y. Reddi and R. B. Sunoj, *ACS Catal.*, 2017, **7**, 530–537.

[8]R. Maji and S. E. Wheeler, *J. Am. Chem. Soc.*, 2017, **139**, 12441–12449.

[9]K. A. Lee, D. Silverio, S. Torker, D. W. Robbins, F. Haeffner, F. W. van der Mei and A. H. Hoveyda, *Nat. Chem.*, 2016, **8**, 768–777.

[10]B. W. Bakr and C. D. Sherrill, *Phys. Chem. Chem. Phys.*, 2016, **18**, 10297–10308.

[11]R. M. Parrish, T. M. Parker and C. D. Sherrill, *J. Chem. Theory Comput.*, 2014, **10**, 4417–4431.

[12]R. M. Parrish and C. D. Sherrill, *J. Chem. Phys.*, 2014, **141**, 044115.

[13]B. Jeziorski, R. Moszynski and K. Szalewicz, *Chem. Rev.*, 1994, **94**, 1887–1930.

[14]E. Papajak, J. Zheng, X. Xu, H. R. Leverentz and D. G. Truhlar, *J. Chem. Theory Comput.*, 2011, **7**, 3027–3034.

[15]T. M. Parker, L. A. Burns, R. M. Parrish, A. G. Ryno and C. D. Sherrill, *J. Chem. Phys.*, 2014, **140**, 094106.

[16]J. L. Whitten, *J. Chem. Phys.*, 1973, **58**, 4496–4501.

[17]B. I. Dunlap, J. W. D. Connolly and J. R. Sabin, *Int. J. Quantum Chem. Symp.*, 1977, **11**, 81.

[18]B. I. Dunlap, J. W. D. Connolly and J. R. Sabin, *J. Chem. Phys.*, 1979, **71**, 3396–3402.

[19]O. Vahtras, J. Almlöf and M. W. Feyereisen, *Chem. Phys. Lett.*, 1993, **213**, 514–518.

[20]R. M. Parrish, L. A. Burns, D. G. A. Smith, A. C. Simmonett, A. E. DePrince, E. G. Hohenstein, U. Bozkaya, A. Y. Sokolov, R. Di Remigio, R. M. Richard, J. F. Gonthier, A. M. James, H. R. McAlexander, A. Kumar, M. Saitow, X. Wang, B. P. Pritchard, P. Verma, H. F. Schaefer, K. Patkowski, R. A. King, E. F. Valeev, F. A. Evangelista, J. M. Turney, T. D. Crawford and C. D. Sherrill, *J. Chem. Theory Comput.*, 2017, **13**,

3185–3197.

[21]F. Weigend, *Phys. Chem. Chem. Phys.*, 2002, **4**, 4285–4291.

[22]F. Weigend, *Phys. Chem. Chem. Phys.*, 2006, **8**, 1057–1065.

[23]T. C. Lillestolen and R. J. Wheatley, *Chem. Comm.*, 2008, **51**, 5909–5911.

[24]G. Knizia, *J. Chem. Theory Comput.*, 2013, **9**, 4834–4843.

[25]K. U. Lao and J. M. Herbert, *J. Phys. Chem. A*, 2012, **116**, 3042–3047.

[26]S. F. Boys and F. Bernardi, *Mol. Phys.*, 1970, **19**, 553–566.

[27]C. Møller and M. S. Plesset, *Phys. Rev.*, 1934, **46**, 618–622.

[28]T. H. Dunning, *J. Chem. Phys.*, 1989, **90**, 1007–1023.

[29]J. Antony and S. Grimme, *J. Phys. Chem. A*, 2007, **111**, 4862–4868.

[30]N. Mardirossian and M. Head-Gordon, *Phys. Chem. Chem. Phys.*, 2014, **16**, 9904–9924.

[31]L. A. Burns, J. C. Faver, Z. Zheng, M. S. Marshall, D. G. A. Smith, K. Vanommeslaeghe, A. D. MacKerell, K. M. Merz and C. D. Sherrill, *J. Chem. Phys.*, 2017, **147**, 161727.

[32]R. M. Parrish, D. F. Sitkoff, D. L. Cheney and C. D. Sherrill, *Chem. Eur. J.*, 2017, **23**, 7887–7890.

[33]Y. Zhao and D. G. Truhlar, *Theor. Chem. Acc.*, 2008, **120**, 215–241.

[34]J. Chai and M. Head-Gordon, *Phys. Chem. Chem. Phys.*, 2008, **10**, 6615.

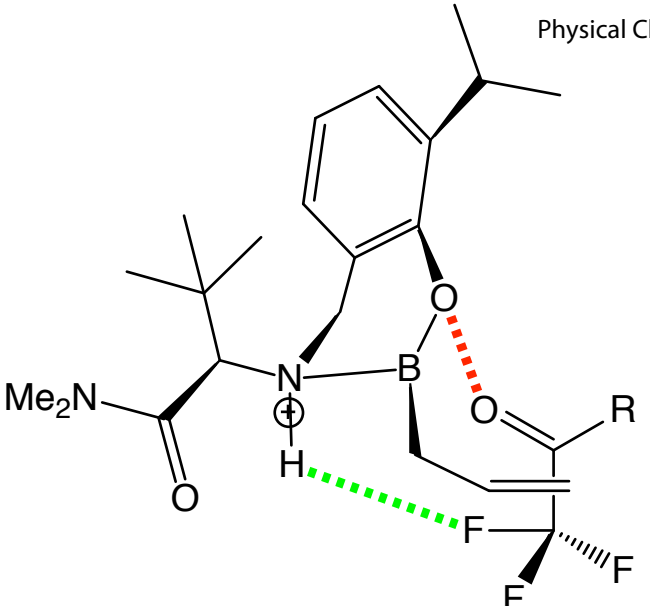

TS II

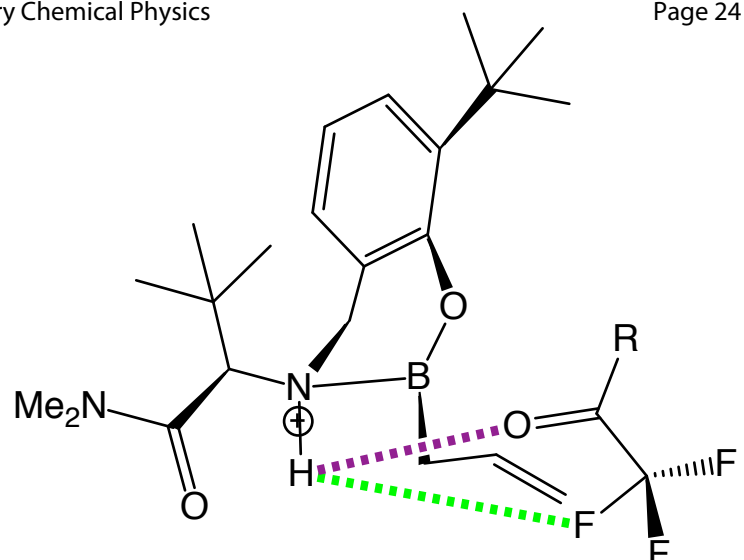

TS IV